Tailoring Mechanical Properties of a Low Carbon Cu-Containing Structural Steel by Two-Step Intercritical Heat Treatment

Xiaohui Xi[1] · Jinliang Wang[1] · Liqing Chen[1] · Zhaodong Wang[1]

Abstract

In this paper, a process of two-step intercritical heat treatment was used to control the amount of retained austenite and nano-scaled precipitates for a low carbon Cu-containing structural steel such that the mechanical properties of this steel can be tailored. In this process, the first step is intercritical annealing and a mixed microstructure can be obtained which contains intercritical ferrite, tempered martensite, fresh martensite and a small amount of retained austenite. The subsequent intercritical tempering was introduced to be beneficial for producing more stable retained austenite at room temperature through secondary enrichment of stabilizers (Mn, Ni). Also, (Nb, V, Mo) (C, N) precipitates were formed during intercritical annealing, while smaller (Nb, V, Mo) (C, N) precipitates and Cu-rich particles with diameter of 5–15 nm were obtained after intercritical tempering. It is due to the contributions from multi-phase microstructure, strain-induced transformation of stable retained austenite and strengthening of nano-scaled precipitates that a combination of high strength, good ductility, low yield to tensile ratio (Y/T ratio) and excellent low-temperature toughness was achieved. The strengthening and toughening mechanism were discussed on the basis of retained austenite formation and interaction between Cu precipitates and the matrix, together with the crack propagation.

Keywords Low carbon Cu-containing steel · Intercritical heat treatment · Retained austenite · Nano-scaled precipitate · Mechanical property

1 Introduction

In order to implement the application in gas pipelines, ship hull, pressure vessel, buildings and offshore structures exposed to arctic environments, there has been a strong drive to develop high strength low alloy (HSLA) steels with a balance of high strength, ductility, excellent low-temperature toughness, good weldability and lower yield to tensile ratio (Y/T ratio). Generally, the production process of the HSLA steels contains chemical composition design and optimization, melting, thermo-mechanical controlled processing (TMCP) and subsequent heat treatment. To meet the requirements for favorable performance, great efforts have been made to optimize the alloy system and production process. However, with the fast development of ultra-high strength steels, there still exist some critical issues to be solved, e.g.

higher Y/T ratio and the intrinsically lower low-temperature toughness for the ultra-high strength steels.

As one of the typical ultra-high strength steels, transformation-induced plasticity (TRIP) steel has been developed to possess a good combination of strength and ductility by TRIP effect of the retained austenite. Meanwhile, numerous studies have been carried out on various alloying steels including conventional TRIP steels [1], medium-Mn steels [2], Q&P steels [3] and 9%Ni cryogenic steels [4]. It is widely accepted that the strength of the steel can be significantly enhanced by martensitic transformation of metastable austenite under external stresses. Also, the stress concentration was released due to the transformation, which delayed the occurrence of necking. Thus, an excellent ductility was obtained. In addition to strength and ductility, it was demonstrated that considerable enhancement of the fracture toughness can also be achieved through the retained austenite, especially by lowering the ductile–brittle transformation temperature (DBTT) [5]. As for the toughening mechanism of retained austenite, however, there still exists controversy remaining to be clarified. It

✉ Liqing Chen
lqchen@mail.neu.edu.cn

1 State Key Laboratory of Rolling and Automation,
Northeastern University, Shenyang 110819, China

has been suggested that the retained austenite served as absorber and promoted a cleaner and ductile martensite, which prevented the crack initiation [6]. Another idea was also proposed that the martensitic transformation of retained austenite occurred at the tip of crack, inhibiting the crack propagation [7]. Therefore, the improved toughness was eventually achieved through preventing crack initiation or changing the crack propagation path. From the above analysis, integration for tailoring strength, ductility and toughness can be successfully realized via retained austenite. Motivated by this, a type of low carbon and low alloy steels with considerable amount of retained austenite was developed which take into account the weldability and energy-saving. In order to obtain stable austenite in low carbon and low alloyed steels, two-step intercritical heat treatment was employed in low carbon (< 0.1 wt%) steels with lean alloying elements ($Mn \leq 2.0$ wt% and $Ni \leq 3.0$ wt%) [8]. In this case, the volume fraction of retained austenite was in the range of 8%–10%. The difference in the amount of retained austenite was controlled primarily by the intercritical heat treatment temperature for given steel, at which reversed austenite transformation and partitioning of alloying elements occurred.

On the other hand, the recovery of dislocations during intercritical heat treatment generally leads to a reduction in strength. Moreover, in order to improve the weldability of steels, ultra-low carbon content ($< 0.1\%$) is generally used in the steel production [9], but it inevitably brings about strength loss. Considering these factors, Cu addition is an effective means to compensate for the loss of strength via precipitation strengthening and has been used to obtain high strength of steels [10]. According to equation [11], the solubility of Cu in ferrite is only 0.5 wt% at 700 °C. Small solubility of Cu in ferrite leads to the formation of Cu precipitates during aging. Upon deformation, the Cu-rich precipitates act as highly efficient obstacles to dislocation motion thereby leading to the enhanced strength of the steels [12]. Additionally, microalloying elements (Nb, V) in the steel may provide effective means for further strengthening via gain refinement and/or precipitation [13].

In this study, a type of high strength low carbon Cu-containing steel was developed by intercritical annealing plus intercritical tempering heat treatment. Microstructural features and mechanical properties of this steel subjected to different heat treatment processes were investigated by scanning electron microscope (SEM) equipped with electron back scattering diffraction (EBSD), transmission electron microscope (TEM) and mechanical properties test. The mechanical properties were tailored by controlling retained austenite and nano-scaled precipitates through adjusting heat treatments. Moreover, the strengthening and toughening mechanism were disclosed in this study.

2 Experimental

A low carbon Cu-containing steel with lean alloying elements was utilized in this study. The nominal chemical composition is 0.08 wt% C, 0.24 wt% Si, 1.0 wt% Mn, 2.5 wt% Ni, 1.5 wt% Cu, 0.55 wt% Mo, 0.54 wt% Cr, 0.032 wt% Nb, 0.05 wt% V, 0.029 wt% Al and Fe balanced. The steel was firstly vacuum-melted into a 50 kg ingot and then forged into rectangle slabs with a cross sectional dimension of 100 mm × 120 mm. The forged slabs were reheated to 1200 °C for 2 h and finally hot rolled to a plate of 24 mm in thickness with multiple passes by a total reduction of 80%. After that, they were air cooled to room temperature.

The heat treatments were carried out in a box resistance furnace. The samples for heat treatment with a dimension of 80 mm × 30 mm × 24 mm were cut along rolling direction. Figure 1 shows the schematic diagram of heat treatment process. The samples were firstly homogenized at 850 °C for 1 h and water quenched to room temperature. The as-quenched steels were then subjected to intercritical annealing. Three intercritical annealing temperatures were designed to produce different microstructures, which were denoted as IA680, IA700 and IA720, respectively. The three groups of annealed steels were finally tempered at 620 °C for 1 h, as designated IT620. Hereafter, the three experimental steels were referred to as IA680-IT620, IA700-IT620 and IA720-IT620, respectively.

Mechanical properties were determined by room temperature tensile test and Charpy impact test. Room temperature tensile test in terms of strength and elongation was conducted on a CMT5105-SANS machine and the crosshead speed was 3 mm/min. The samples for tensile test were machined with a gauge length of 25 mm and diameter of 5 mm along the rolling direction. Charpy V-notch
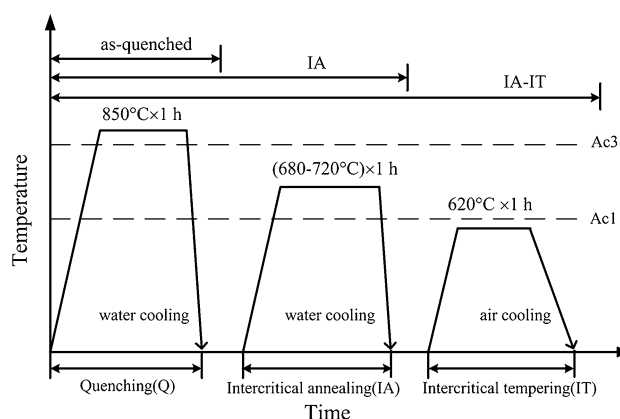
Fig. 1 Schematic of heat treatments for this low carbon Cu-containing steel

(CVN) impact test was conducted by adopting standard specimens of 10 mm × 10 mm × 55 mm at − 40 °C.

The microstructure features and nano-precipitates were carefully examined by scanning electron microscope (SEM) and transmission electron microscope (TEM). The SEM observation was performed on a ZEISS ULTRA-55 field emission scanning electron microscope (FE-SEM) at an acceleration voltage of 15 kV. The samples were etched for approximately 30–40 s with 4 vol% nital solution. The TEM studies were conducted by FEI Tecnai G^2 F20 TEM at an acceleration voltage of 200 kV. The thin foils (φ3 mm in diameter) for TEM observation were firstly mechanically ground down to ~ 50 μm thickness, and then twin-jet polished in a solution of 12.5 vol% perchloric acid and 87.5 vol% alcohol. To characterize the distribution and morphology of the retained austenite, electron back scatter diffraction (EBSD) test was carried out at an acceleration voltage of 20 kV and the scanning step size was 0.15 μm. The EBSD samples were prepared by electro-polishing in the same solution as that for TEM observation. The polishing process was carried out for 20 s at a voltage of 18 V to relieve the surface stress. The XRD profiles of the retained austenite was measured in a Smart Lab 9 kW X-ray diffractometer with CuKα radiation at a scanning speed of 4°/min. The volume fractions of retained austenite under various heat treatments were estimated based on the integrated intensities of $(200)_\alpha$, $(211)_\alpha$, $(200)_\gamma$, $(220)_\gamma$ and $(311)_\gamma$ diffraction peaks. The procedure of XRD samples preparation was the same as that for EBSD measurement. Compositional analysis of different phases was carried out by energy dispersive X-ray spectroscopy (EDXS).

3 Results

3.1 Mechanical Properties

Mechanical properties in terms of strength, total elongation, Y/T ratio and low-temperature toughness were summarized in Table 1 for this low carbon Cu-containing steel after various heat treatments. Among these, IA700-IT620 has been

demonstrated in previous study [14]. After the intercritical annealing was introduced to the IA700-IT620, the steel with a combination of high strength, good elongation, low Y/T ratio and excellent low-temperature toughness was obtained. This is attributed to the multiphase microstructure and deformation-induced transformation of the retained austenite. It revealed that the intercritical annealing played a dominant role in enhancing mechanical properties by introducing retained austenite. Therefore, the amount of retained austenite could be controlled by adjusting intercritical annealing heat treatments, and accordingly the mechanical property can be tailored. In this study, the mechanical properties at annealing temperature of 680 °C and 720 °C were compared with those at annealing temperature of 700 °C, and optimum technology was obtained.

As listed in Table 1, the quenched steel exhibited high yield strength (~ 980 MPa), ultra-high tensile strength (~ 1287 MPa) and lower Y/T ratio (~ 0.76), but a low total elongation (~ 13.2%) and a relatively poor low-temperature toughness (~ 100 J at − 40 °C). After intercritical annealing, the yield strength and tensile strength dropped dramatically, while the total elongation and low-temperature toughness were increased to some extent. For IA680, the yield strength, tensile strength and Y/T ratio were ~ 773 MPa, ~ 949 MPa and 0.81, respectively. Also, a higher total elongation of ~ 18.6% and a considerable high low-temperature toughness of ~ 182 J at − 40 °C were obtained. In contrast, the yield strength of IA700 was decreased to ~ 680 MPa, while the yield strength of IA720 was enhanced up to ~ 863 MPa. In these cases, the tensile strengths reached ~ 1012 MPa and ~ 1091 MPa for IA700 and IA720, respectively. Y/T ratio, ductility as well as Charpy impact energy at − 40 °C all exhibited decline to some degrees. For the intercritical annealing and intercritical tempering heat treatment, when IA680 and IA700 were treated at the same intercritical tempering temperature, there were ~ 47 MPa and ~ 150 MPa increase in yield strength compared to the first-step annealing treatment, but a decrease of ~ 75 MPa for IA720. The tensile strength separately decreased to ~ 922 MPa, ~ 961 MPa and ~ 877 MPa for IA680-IT620, IA700-IT620 and IA720-IT620. The Y/T ratio was increased by tempering, but it

**Table 1** Mechanical properties of the steels after various heat treatments

Processes	YS (MPa)	TS (MPa)	Y/T ratio	TEL (%)	CVN/J (− 40 °C)			
					CVN 1	CVN 2	CVN 3	Average value
As-quenched	980 ± 20	1287 ± 2	0.76 ± 0.1	13.2 ± 0.9	108	94	98	100
IA680	773 ± 3	949 ± 2	0.81	18.6 ± 1.8	190	180	176	182
IA700	680 ± 10	1012 ± 1	0.67 ± 0.1	18.1 ± 1.3	128	137	128	131
IA720	863 ± 15	1091 ± 21	0.79 ± 0.3	14.6 ± 1.4	116	112	116	115
IA680-IT620	820 ± 2	922 ± 22	0.89 ± 0.1	18.5 ± 1.5	227	207	216	217
IA700-IT620	830 ± 5	961 ± 0.5	0.86	22.2 ± 0.3	216	225	216	219
IA720-IT620	788 ± 12	877 ± 11	0.90	20.6 ± 1.0	198	222	184	201

still remained at a desired level less than 0.90. The total elongation remained to be ~18.5% for IA680-IT620, while there was a slight increase in the total elongations for IA700-IT620 and IA720-IT620. Additionally, it is worth noting that the Charpy impact energy at −40 °C was enhanced largely to a high level of more than 200 J after the annealed steels were intercritically tempered at 620 °C.

3.2 Microstructure Features

SEM images of this steel subjected to different heat treatments are shown in Fig. 2. The microstructure presented in Fig. 2a is typical lath martensite obtained by water quenching after the hot-rolled steel was austenitized at 850 °C for 1 h. It can be seen that there existed a initially fine martensite structure, which was beneficial for microstructure refinement in the subsequent heat treatments. Figure 2b–d showed the microstructures of IA680, IA700 and IA720, respectively. For IA680, tempered martensite was dominantly dispersed

with some fine freshly formed martensite and intercritical ferrite, as observed in Fig. 2b. The fresh martensite was distributed together with intercritical ferrite, from which it can be inferred that the newly formed martensite and ferrite came from the same reverted structure. Also, some of tempered microstructure still remained lath-like morphology due to lower intercritical annealing temperature. As shown in Fig. 2c, the finer microstructure of IA700 can be characterized by intercritical ferrite, tempered martensite, fresh martensite or retained austenite along grain boundaries, which were uniformly dispersed in the matrix. After intercritical annealing at a higher temperature of 720 °C, more and coarser fresh martensite with intercritical ferrite was obtained as seen in Fig. 2d. The intercritical ferrite stemmed from lath martensite due to redistribution of alloying elements, and thus inherited lath-like structure of lath martensite. As a result, it was located together with fresh lath martensite after intercritical annealing. The tempered microstructure of this steel soaked at 620 °C after
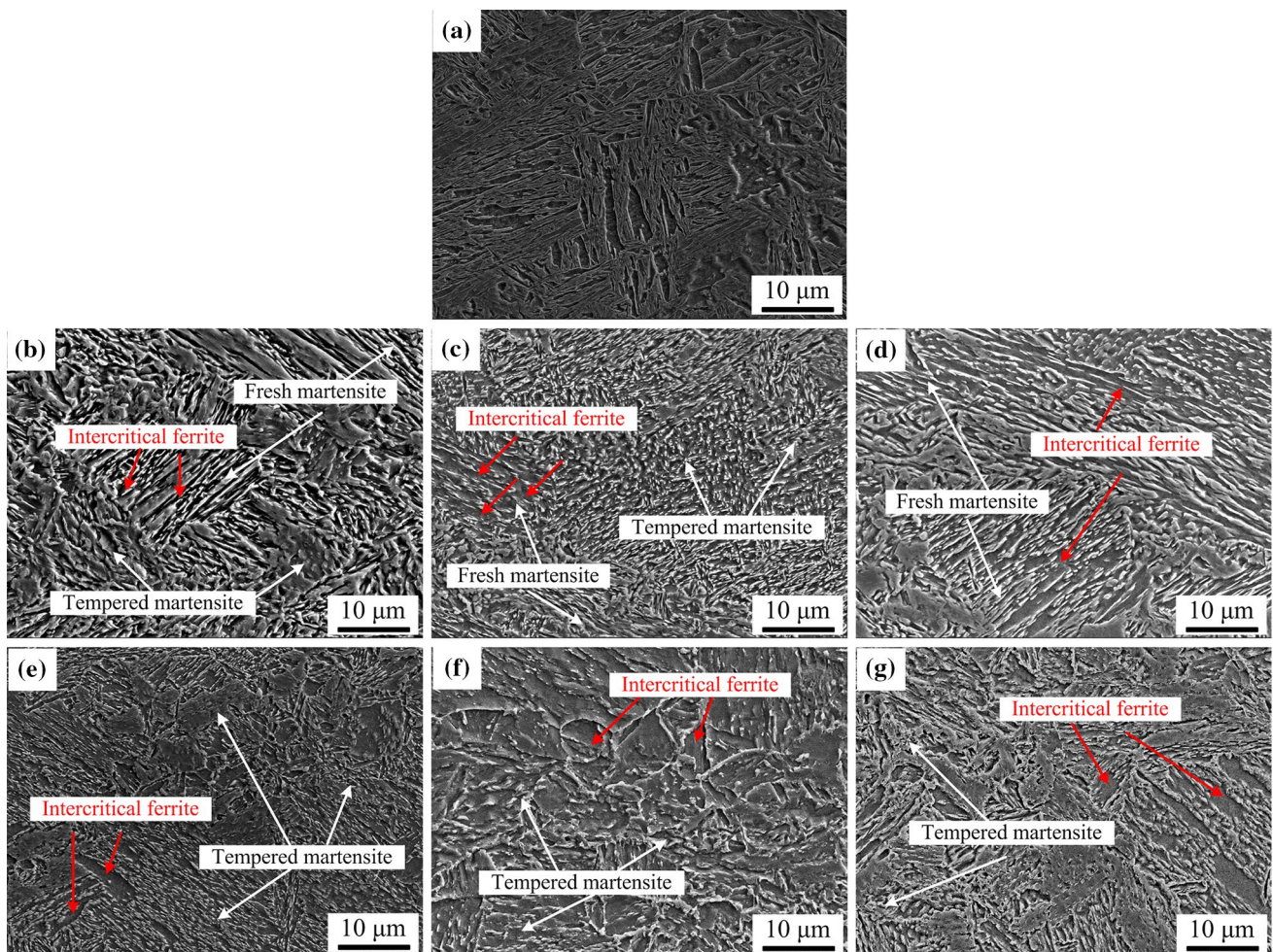
Fig. 2 SEM micrographs of the low carbon Cu-containing steel subjected to various heat treatments: **a** as-quenched, **b** IA680, **c** IA700, **d** IA720, **e** IA680-IT620, **f** IA700-IT620, **g** IA720-IT620

intercritical annealing at 680 °C, 700 °C and 720 °C were presented in Fig. 2e–g, respectively. A multi-phase microstructure consisting of intercritical ferrite, tempered martensite and retained austenite was obtained in these three groups of experimental steels. At this stage, the tempered martensite and newly formed martensite during intercritical annealing experienced a process of recovery. Among these, fine tempered microstructure was dispersedly and homogeneously distributed in the matrix of IA680-IT620 as shown in Fig. 2e. Moreover, most of the ferrite existed in form of laminar- or lath-like morphology. For IA700-IT620 and IA720-IT620, the fine intercritical ferrite coalesced with each other and finally existed as blocky (Fig. 2f, g). What is more, the boundaries of the microstructure became ambiguous due to recovery. Additionally, the IA720-IT620 adopted the lath-like feature of original martensite produced by intercritical annealing as seen in Fig. 2g.

3.3 Characterization of Retained Austenite

The morphology of retained austenite and distribution were characterized by EBSD technique. Figure 3 showed the band contrast (BC) maps with face centered cubic (FCC) phase for this steel heat-treated by different processes. For IA680, only a trace amount of film-like retained austenite was found in the matrix as seen from Fig. 3a. As the intercritical annealing temperature was increased to 700 °C (IA700), much more retained austenite was observed in the matrix (Fig. 3b) in comparison with IA680. The retained austenite

with film-like morphology was mainly distributed between matrix laths, while the blocky ones were located at grain boundaries. For IA720, a similar observation was made with IA680 as indicated in Fig. 3c. After subsequent intercritical tempering at 620 °C, the volume fractions of the retained austenite in the matrix exhibited an increase to some extent for IA680, IA700 and IA720, as shown in Fig. 3d–f respectively. Among these, a larger amount of retained austenite was observed in IA700-IT620 steel (Fig. 3e) as compared with IA680-IT620 and IA720-IT620 steels (Fig. 3d, f). It was also noted that the retained austenite was mainly dispersed at darker areas. According to a previous study [15], darker areas for gray phases were generally considered to be martensite with high density of dislocations and high concentration of alloying elements. This demonstrated that the retained austenite was enriched with high alloying elements and formed along with martensite.

The retained austenite was quantitatively studied by using XRD analysis. Figure 4a presented XRD spectra of this steel after various heat treatments, and the corresponding volume fractions of retained austenite were plotted in Fig. 4b. The volume fractions of retained austenite were estimated to be 2.4% and 3.0%, respectively, for IA680 and IA720. There was no much difference for these two annealing temperatures. When the annealed steels were subsequently tempered at 620 °C, the volume fraction of retained austenite was increased to 5.0% and 6.4%, respectively. However, for IA700, the volume fraction of retained austenite was as high as 9.4%. By secondary tempering
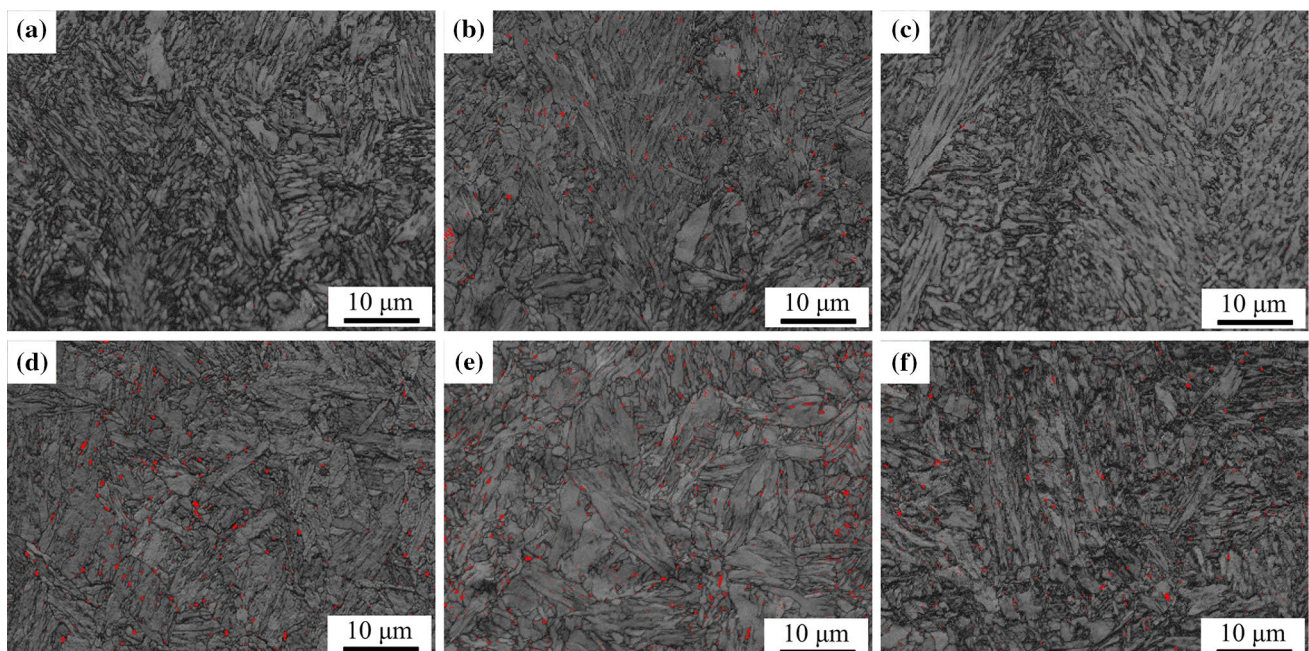
Fig. 3 EBSD images of low carbon Cu-containing steel subjected to various heat treatments: **a** IA680, **b** IA700, **c** IA720, **d** IA680-IT620, **e** IA700-IT620, **f** IA720-IT620. The red part corresponds to FCC retained austenite. (Color figure online)

Fig. 4 XRD spectra (**a**) and measured austenite volume fractions (**b**) of steels subjected to various heat treatments
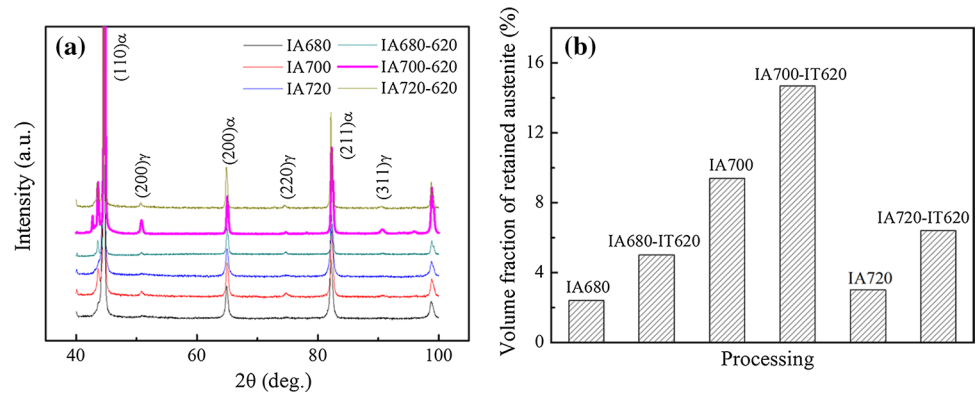

at 620 °C, the volume fraction of retained austenite was further increased to a higher level of 14.7%. These results indicated that both intercritical annealing and tempering processes were essential to obtain a certain amount of retained austenite at room temperature.

Figure 5 shows the TEM images of the matrix and retained austenite for IA700-IT620, and the chemical compositions of different phases were determined by EDXS equipped with TEM. The contents of Mn, Ni and Cu in the retained austenite were about 2.44%, 1.21% and 0.37% (in wt%) respectively, while the alloy content in matrix was 0.8%Mn, 1.0% Ni and 0.8% Cu (in wt%). In addition, the retained austenite had a carbon concentration of ~ 0.986 wt% according to the formula [16]. It is known that the average carbon content in the matrix is ~ 0.08 wt%. This indicated that the retained austenite was enriched with Mn, Ni and C elements beneficial to stabilize retained austenite, while Cu was mainly precipitated in the matrix.

3.4 Nano-scaled Precipitates

Besides the considerable volume fraction of retained austenite, precipitates with various sizes were also observed by TEM, as shown in Fig. 6. Figure 6a–c presented the precipitation features of IA680, IA700 and IA720, respectively. A number of precipitates with average diameter of 7 nm were distributed in the matrix of this steel subjected to different intercritical annealing processes, which were determined to be complex carbonitride particles (Nb, Mo, V) (C, N) by EDXS analysis in TEM (Fig. 6g). It should be noted that no Cu-enriched particles were observed in the steel after intercritical annealing. This was due to the fact that Cu-enriched particles were generally precipitated at temperature lower than 700 °C, thus the Cu existed in the matrix mainly as solid solution without precipitating when soaking at intercritical annealing temperature. Moreover, at the cooling stage of intercritical annealing, the precipitation of Cu particles was inhibited resulted from high cooling

Fig. 5 TEM images showing the chemical composition in matrix and retained austenite of IA700-IT620
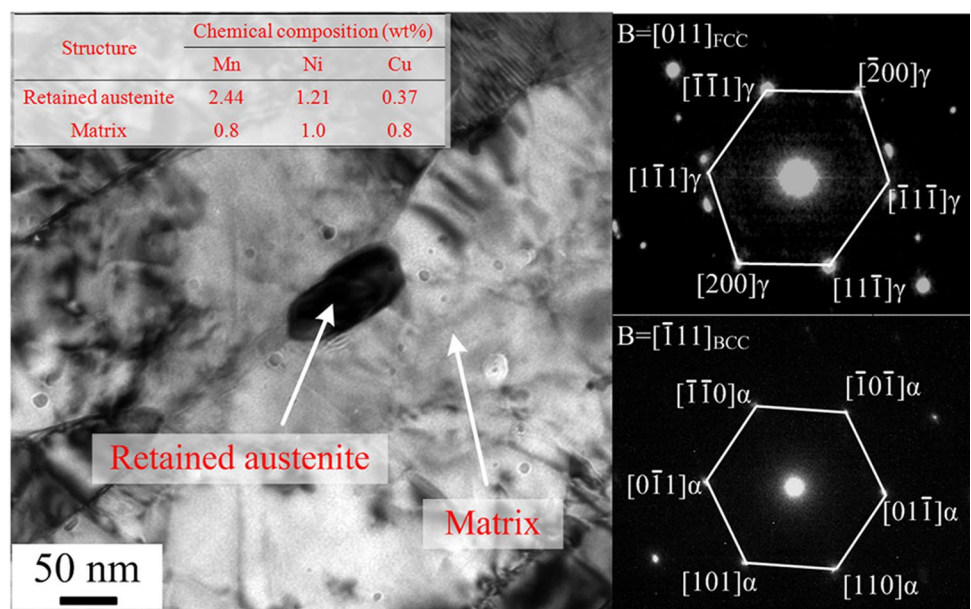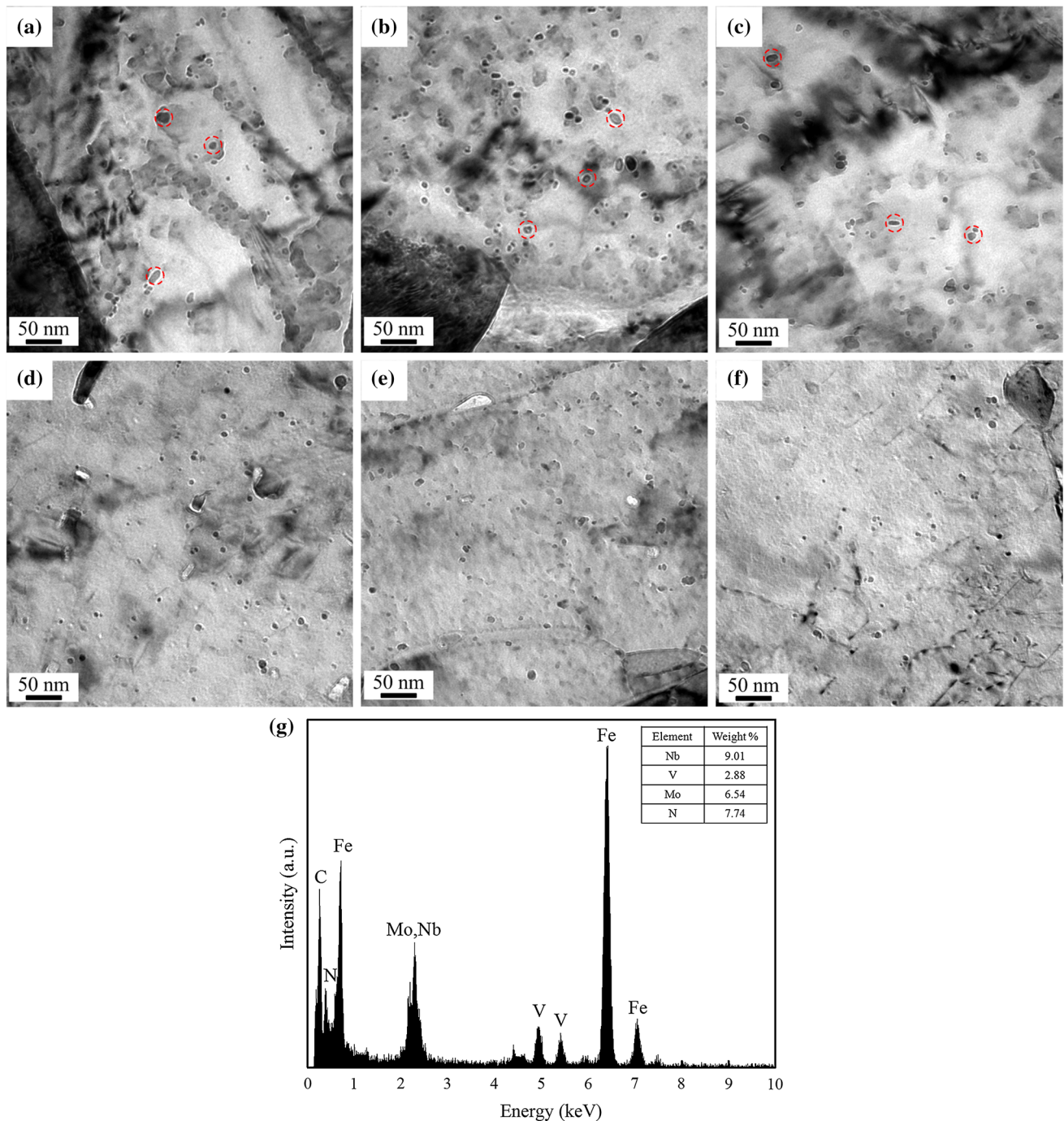
Fig. 6 TEM images of the low carbon Cu-containing steel subjected to various heat treatments: **a** IA680, **b** IA700, **c** IA720, **d** IA680-IT620, **e** IA700-IT620, **f** IA720-IT620, **g** EDXS of precipitates with red dotted circles in **a**–**c**. (Color figure online)

rate. Figure 6d–f showed the precipitation behavior of this steel after intercritical annealing and intercritical tempering at 620 °C. In addition to the larger precipitates formed at the stage of intercritical annealing, some finer precipitates with mean size of 3 nm were also present in the matrix. These precipitates were considered to be (Nb, Mo, V) (C, N) formed during tempering. What is more, the Cu-rich precipitates with a diameter range of 5–15 nm were dispersedly distributed in the matrix. Some precipitates exhibited almost spherical in shape, while other larger ones appeared to be elliptic with aspect ratio of about 1.9. This result suggests that large amount of nano-scaled carbonitride and Cu-rich precipitates are resulted from tempering and they would exert strengthening effect on the steel matrix.

Given that the strengthening effect of Cu-rich precipitate strongly depends on its crystal structure, high resolution TEM (HRTEM) was employed to characterize its crystal features. Figure 7 showed the HRTEM images of Cu-rich precipitates with a diameter of ~ 5 nm in IA700-IT620. The corresponding fast Fourier transform (FFT) was conducted in Cu precipitate (rectangle I in Fig. 7a) and its surrounding structure (rectangle II in Fig. 7a), as presented in Fig. 7b, c, respectively. The results show that Cu-rich precipitate was characterized by "distorted" face-centered cubic (fcc) crystal structure. Researcher agreed that fcc Cu was transformed from bcc and 9R structure, and has lost coherence with the bcc matrix [17]. Accordingly, the strengthening effect exhibited a decrease along with the change of crystal structure. The rectangle II possessed B2-ordered structure and this was considered to be a shell existing at the interface between α-Fe matrix and Cu precipitate. Although relatively lower strengthening effect of fcc Cu precipitate was unexpected, the precipitation strengthening effect from fcc Cu and carbonitride was still enough to resist the softening of matrix during tempering and make the steel strength much higher.

4 Discussion

It is well known that the martensite as initial microstructure was firstly obtained by quenching to room temperature. The quenched steel was then reheated to two-phase (α + γ) region for intercritical annealing. When soaking at α + γ region, the diffusion of elements such as C, Mn, Ni, Cu from matrix to austenite can be found due to the difference in solid solubility [8]. During intercritical annealing, some amount of martensite retransformed to austenite, which was called austenite reverted transformation (ART) [18]. The amount of reverted austenite was strongly dependent on the annealing temperature. In the present work, the volume fractions of austenite

at different intercritical annealing temperatures as measured by high temperature XRD (HT-XRD) and room temperature XRD (RT-XRD) were shown in Fig. 8. For IA680, a small amount of reverted austenite was preferentially formed, and the volume fraction was estimated to be 20.4%. However, only 2.4% was kept to room temperature due to a considerably low diffusion rate of austenite stabilizers. By comparison, the volume fractions of the reverted austenite in IA700 and IA720 were increased to 41.3% and 57.5% respectively, which presented approximately linear increase. As the annealed steels cooled down to room temperature, a larger amount of retained austenite was obtained for IA700. The volume fraction of retained austenite was estimated to be as high as 9.4%. It can be attributed to a dual effect of a high austenite stabilizers concentration and a small grain size [19]. For IA720, the amount of retained austenite dramatically decreased to about 3.0% due to slighter enrichment of alloying elements in reverted austenite, although the volume
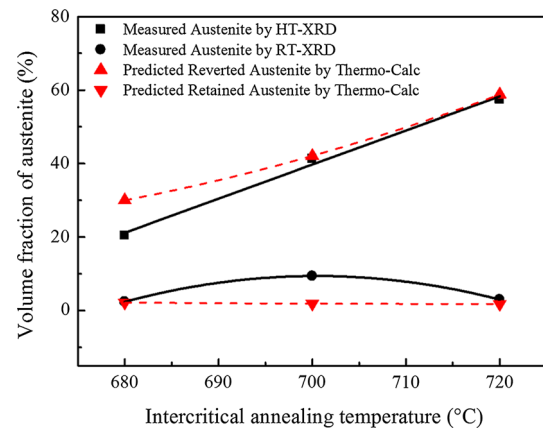
Fig. 8 Volume fractions of austenite as a function of intercritical annealing temperature as measured by XRD and predicted by Thermo-Calc software in the low carbon Cu-containing steel
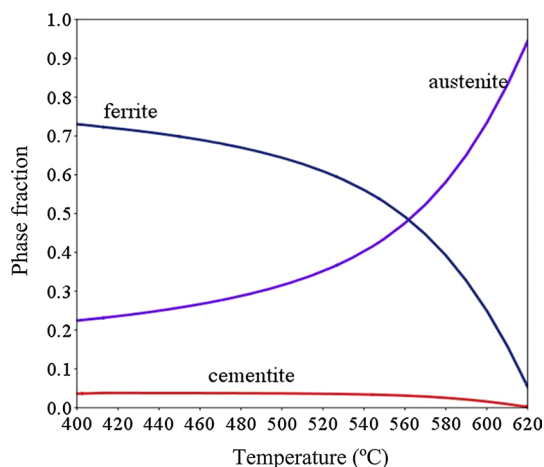

Fig. 7 HRTEM images of Cu precipitate in IA700-IT620: **a** HRTEM image, **b**, **c** are FFT patterns of the selected rectangle I and II in a, respectively
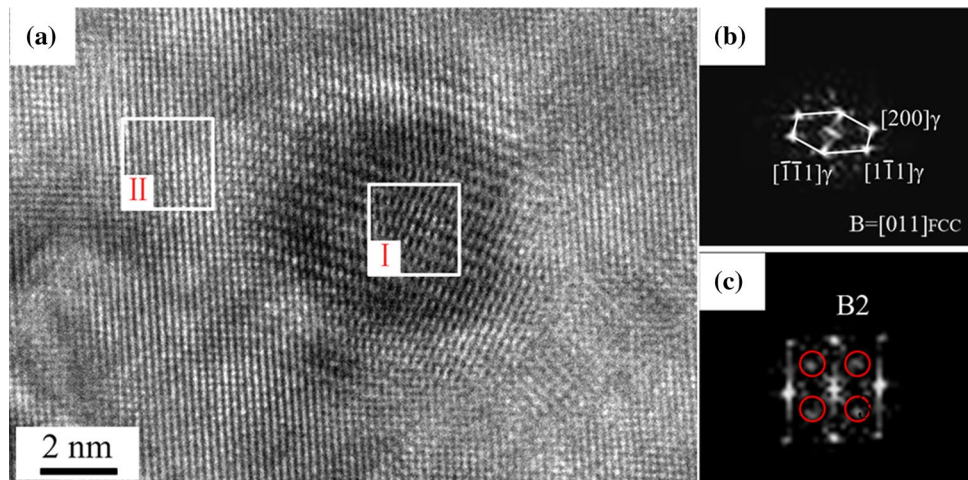
fraction of reverted austenite was higher. Thermo-Calc software was employed to predict the volume fractions of austenite, and the results were plotted by dotted lines in Fig. 8. It can be found that the predicted results had a good match with the measured ones, which indicated that the Thermo-Calc can be used to guide the experimental process and predict experimental result.

The thermodynamics of retained austenite stabilization was discussed by Thermo-Calc calculations based on TCFE9 database for intercritical heat treatment. Take IA700 for example, the equilibrium chemical composition of reverted austenite was calculated to be Fe–0.2C–0.2Si–0.51Mn–0.4 Mo–0.69Cr–1.8Cu–5Ni–0.02Al–0.003V (wt%). When the annealed steel was subjected to tempering at 620 °C, it is supposed that austenite formed only in enriched martensite or preformed austenite in the intercritical annealing process. Based on the above assumption and equilibrium chemical composition, the volume fraction of austenite subjected to tempering was determined to be 26.6%, and the corresponding chemical composition was Fe–0.22C–0.19Si–1.34Mn–0 .05Mo–0.35Cr–1.89Cu–11.23Ni–0.03Al–0.001V (in wt%). According to an empirical formula [20], the martensite start temperature (Ms) of austenite was calculated to be 157 °C. By using K–M equation [21], the volume fraction of retained austenite was estimated to be only 2.5% for IA700-IT620, which was much less than 14.7% from XRD results. This was due to the calculation from Thermo-Calc based on the single-point equilibrium. The cementite was inevitable to precipitate during intercritical tempering at 620 °C as demonstrated in Fig. 9, which consumed the carbon element and lowered the stability of austenite. However, the carbon diffusion from matrix to austenite has been completed during actual intercritical annealing heat treatment [22]. The reverted aus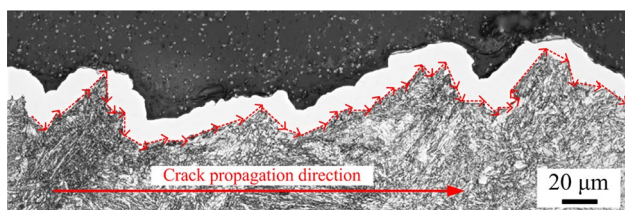tenite formed in the tempering process was stabilized by further enrichment of austenite stabilizers such as Ni and Mn, thus more stable austenite was obtained.

It has been widely accepted that both the strength and ductility can be remarkably improved through strain-induced transformation of retained austenite. In this work, the strength remained at a high level, although the softening effect was present during heat treatments. In addition to the effect of retained austenite, the high strength was also attributed to Nb, V, Mo carbonitride and Cu precipitation strengthening.

Precipitates containing Nb and V were preliminarily formed during hot rolling, in which a larger size was obtained due to high temperature. Although it was found that the coarsening kinetics of precipitates can be inhibited by Mo addition [23], here its contribution to the strength was considered to be little and will not be discussed. The complex precipitates (Nb, V, Mo) (C, N) formed in the intercritical annealing had an average diameter of 7 nm, which strengthened the matrix by pinning the dislocations. The subsequent tempering introduced some amount of finer (Nb, V, Mo) (C, N) precipitates with size of less than 5 nm and dispersed Cu-rich particles with an average size of 10 nm. It has been suggested that the carbonitride precipitation strengthening is related to the interaction between dislocations and precipitates. Generally, the carbonitride is much harder than the iron matrix, and the dislocation moves bypassing the particles. Thus, the strengthening can be considered to be Orowan mechanism [24]. However, Cu precipitation strengthening mechanism is much complex due to its varying crystal structure during heat treatments. The Cu precipitation strengthening is highly dependent on the coherency strain, elastic modulus, chemical composition of Cu clusters, interaction with dislocations, etc. In this study, most of Cu precipitates existed as fcc Cu incoherent with the matrix. It is indicated that the strain strengthening is derived from a small residual strain field around non-coherent precipitates [25]. Thus, it can be neglected. Also, it is proposed a theory that the interaction between dislocations and Cu precipitates with a lower elastic modulus than the matrix helps to increase shear yield stress [26]. Since fcc Cu precipitate consists of almost pure Cu, however, the elastic modulus strengthening is suggested to be less effective [25]. Therefore, Cu precipitation strengthening in this study was mainly focused on the interaction between Cu particles and dislocations. In contrast to carbonitride, the Cu particles are softer than the iron matrix and the dislocation can cut through rather than bypass the particles [27]. So the strengthening mechanism is completely different from Orowan mechanism. Nakashima et al. have proved that the strengthening effect of Cu precipitates is dependent on particle size and spacing [28]. Furthermore, the influence of co-addition alloying elements on strength was compared

Fig. 9 Phase fractions as a function of temperature predicted by Thermo-Calc software in the low carbon Cu-containing steel

Fig. 10 Crack propagation path of the cross-sectional area of the impact specimens tested at − 40 °C for IA700-IT620 steel

and it was found that the stable B2 shell contributed to the significant improvement in strength, which can be interpreted by the fact that B2 shell enriched with Ni, Mn, Al gave rise to a low interface energy, and hence a smaller size and a higher number density of Cu-rich precipitates [29].

The excellent low-temperature toughness in Charpy impact test was closely related to the multi-phase microstructure and stable retained austenite. On the one hand, it was indicated that the grain size can be further refined by more soft and ductile phase introduced by intercritical annealing and tempering [30], which helped to inflect the crack propagation and also reduce the average length of unit crack paths. Also, the ductile second phase oriented for easy slip may be beneficial for toughness [31]. On the other hand, the stable retained austenite can provide a continuous strain-induced transformation effect and effectively hinder crack propagation. Therefore, the enhancement of low temperature toughness was achieved through affecting crack propagation. In this study, the crack propagation paths in the cross-sectional area of Charpy impact specimens tested at − 40 °C were given in Fig. 10. The crack propagation path in IA700-IT620 was frequently inflexed. The average length of unit crack path was only 16 μm. As a result, more energy would be consumed during the crack propagation, thus leading to a significant improvement of the low-temperature toughness.

From the aforementioned analysis, the (Nb, V, Mo) (C, N) precipitates and Cu-rich particles as well as considerable amount of retained austenite were successfully introduced to the microstructure by intercritical annealing and subsequent tempering heat treatment. By combination of precipitation strengthening of nano-scaled precipitates and strain-induced transformation of stable retained austenite, excellent mechanical properties in terms of strength, ductility and low-temperature toughness were achieved in this Cu-containing low carbon low alloyed steel. It is a promising pathway to simultaneously adopt Cu precipitation strengthening and retained austenite toughening in alloyed steels to achieve a combined effect of strength, ductility and toughness.

5 Conclusions

A low carbon Cu-containing steel was developed by intercritical annealing and tempering heat treatment. Microstructure features and mechanical properties of this steel were tailored by adopting different intercritical annealing temperatures. The conclusions can be drawn as follows.

(1) A multi-phase microstructure consisting of intercritical ferrite, tempered martensite as well as considerable amount of retained austenite was obtained in the low carbon Cu-containing steel after intercritical annealing and tempering. The retained austenite enriched with Mn, Ni and C elements was stable enough to benefit the enhancement of strength, ductility and low-temperature toughness by means of strain-induced transformation effect.

(2) Complex precipitates (Nb, V, Mo) (C, N) and Cu-rich particles were formed during intercritical annealing and tempering process. These nano-scaled precipitates guaranteed the high strength of the softening matrix in the experimental steels through interacting with dislocations.

(3) The combined contribution of multi-phase microstructure, stable retained austenite and nano-scaled precipitates is the underlying basis for high strength, low Y/T ratio, good ductility and excellent low temperature toughness. A high performance low carbon low alloyed steel with yield strength greater than 800 MPa, tensile strength greater than 900 MPa, low Y/T ratio of 0.86, total elongation of ∼22% and superior low temperature toughness of ∼219 J at − 40 °C can be obtained by annealing at 700 °C plus tempering at 620 °C.

References

1. H.K.D.H. Bhadeshia, D.V. Edmonds, Metall. Trans. A **10**, 895 (1979)
2. Z.H. Cai, H. Ding, R.D.K. Misra, Z.Y. Ying, Acta Mater. **84**, 229 (2015)
3. E. De Moor, S. Lacroix, A.J. Clarke, J. Penning, J.G. Speer, Metall. Mater. Trans. A **39**, 2586 (2008)
4. N. Nakada, J. Syarif, T. Tsuchiyama, S. Takaki, Mater. Sci. Eng. A **374**, 137 (2004)
5. J.I. Kim, H.J. Kim, J.W. Morris, Metall. Trans. A **15**, 2213 (1984)
6. B. Fultz, J. Kim, Y. Kim, H. Kim, G. Fior, J. Morris, Metall. Trans. A **16**, 2237 (1985)
7. G. Ghosh, G.B. Olson, Acta Mater. **42**, 3361 (1994)

8. Z.J. Xie, G. Han, W.H. Zhou, C.Y. Zeng, C.J. Shang, Mater. Charact. **113**, 60 (2016)
9. B.A. Graville, *Cold Cracking in Welds in HSLA* (ASM, Metal Park, OH, 1978)
10. S. Vaynman, D. Isheim, R. Prakash Kolli, S.P. Bhat, D.N. Seidman, M.E. Fine, Metall. Mater. Trans. A **39**, 363 (2008)
11. H.A. Wriedt, L.S. Darken, Trans. Metall. Soc. AIME **218**, 30 (1960)
12. M.E. Fine, D. Isheim, Scr. Mater. **53**, 115 (2005)
13. G.K. Tirumalasetty, M.A. van Huis, C.M. Fang, Q. Xu, F.D. Tichelaar, D.N. Hanlon, J. Sietsma, H.W. Zandbergen, Acta Mater. **59**, 7406 (2011)
14. X.H. Xi, J.L. Wang, X. Li, L.Q. Chen, Z.D. Wang, Metall. Mater. Trans. A **50**, 2912 (2019)
15. A.A. Mohsen, M. Goodarzi, S. Kheirandish, ISIJ Int. **48**, 1251 (2008)
16. G. Gao, H. Zhang, X. Gui, P. Luo, Z. Tan, B. Bai, Acta Mater. **76**, 425 (2014)
17. Y.U. Heo, Y.K. Kim, J.S. Kim, J.K. Kim, Acta Mater. **61**, 519 (2013)
18. Y. Ma, Mater. Sci. Technol. **33**, 1713 (2017)
19. J. Chiang, B. Lawrence, J.D. Boyd, A.K. Pilkey, Mater. Sci. Eng. A **528**, 4516 (2011)
20. A.A. Gorni, *Steel Forming and Heat Treating Handbook* (São Vicente SP, Brazil, 2015), p. 37
21. E.D. Moor, D.K. Matlock, J.G. Speer, M.J. Merwin, Scr. Mater. **64**, 185 (2011)
22. W.H. Zhou, H. Guo, Z.J. Xie, X.M. Wang, C.J. Shang, Mater. Sci. Eng. A **587**, 365 (2013)
23. F.M. Liu, J.J. Wang, Y.J. Liu, R.D.K. Misra, C.M. Liu, J. Iron. Steel Res. Int. **23**, 559 (2016)
24. E. Orowan, *Discussion in the symposium on internal stress in metals and alloys* (Institute of Metals, London, 1948)
25. K. Osamura, H. Okuda, S. Ochiai, M. Takashima, K. Asano, M. Furusaka, K. Kishida, F. Kurosawa, ISIJ Int. **34**, 359 (1994)
26. K.C. Russell, L.M. Brown, Acta Mater. **20**, 969 (1972)
27. J. Friedel, *Dislocations* (Pergammon Press, New York, 1964), p. 454
28. K. Nakashima, Y. Futamura, T. Tsuchiyama, S. Takaki, Trans. Iron Steel Inst. Jpn. **42**, 1541 (2002)
29. Y. Wen, Y. Li, A. Hirata, Y. Zhang, T. Fujita, T. Furuhara, C. Liu, A. Chiba, M.W. Chen, Acta Mater. **61**, 7726 (2013)
30. M. Niikura, J.W. Morris, Metall. Trans. A **11**, 1531 (1980)
31. A. Misra, R. Gibala, R.D. Noebe, Intermetallics **9**, 971 (2001)